

COLUMBUS: Automated Discovery of New Multi-Level Features for Domain Generalization via Knowledge Corruption

Ahmed Frikha^{1,2,3}, Denis Krompaß^{1,2}, Volker Tresp^{2,3}

¹Siemens AI Lab

²Siemens Technology

³Ludwig Maximilian University of Munich
ahmed.frikha@siemens.com

Abstract

Machine learning models that can generalize to unseen domains are essential when applied in real-world scenarios involving strong domain shifts. We address the challenging domain generalization (DG) problem, where a model trained on a set of source domains is expected to generalize well in unseen domains without any exposure to their data. The main challenge of DG is that the features learned from the source domains are not necessarily present in the unseen target domains, leading to performance deterioration. We assume that learning a richer set of features is crucial to improve the transfer to a wider set of unknown domains. For this reason, we propose COLUMBUS, a method that enforces new feature discovery via a targeted corruption of the most relevant input and multi-level representations of the data. We conduct an extensive empirical evaluation to demonstrate the effectiveness of the proposed approach which achieves new state-of-the-art results by outperforming 18 DG algorithms on multiple DG benchmark datasets in the DOMAINBED framework.

1 Introduction

Deep learning models have achieved tremendous success when applied to independent and identically distributed (i.i.d.) data. However, in real-world applications, domain drifts, i.e., distribution shifts between training and test data, are commonly encountered. For instance, data distributions might differ from one hospital to another (Dou et al. 2019), and from one production plant to another. Similarly, computer vision models deployed in self-driving cars are exposed to different urban and rural environments in different countries with changing weather conditions (Yue et al. 2019) and object poses (Alcorn et al. 2019).

Approaches to make machine learning models resilient to these data distribution changes were extensively studied for different domain shift settings. For example, several domain adaptation methods were developed to address the case where, besides the data from the source domain(s), a set of labeled (Wang and Deng 2018) or unlabeled (Wilson and Cook 2020) data is available from a specific target domain.

However, in real-world scenarios, collecting data from the target domain(s) is often slow, e.g., a new hospital or production site, expensive, or even infeasible, e.g., collecting images from every street of every country in the context of self-driving cars. Sometimes, the target domains cannot be known beforehand.

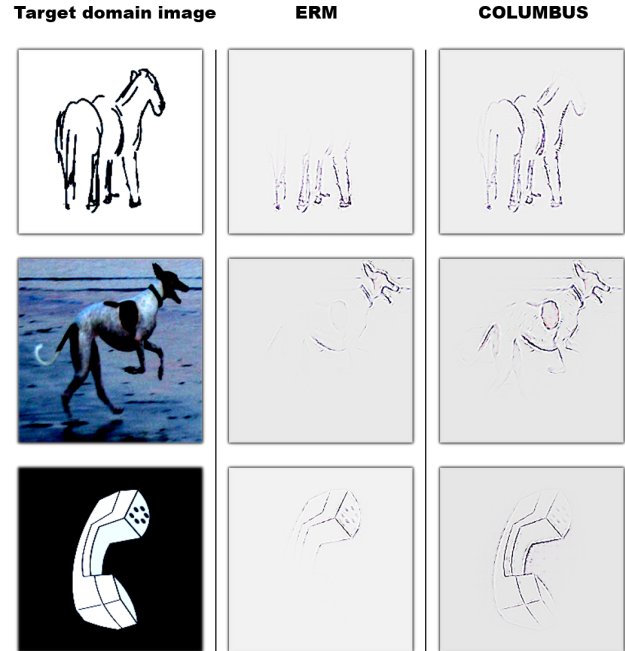


Figure 1: Visualization of relevance maps computed with GuidedGrad-CAM (Selvaraju et al. 2017) for ERM and COLUMBUS using images from the target domains, PACS Sketch, VLCS VOC and OfficeHome Clipart. COLUMBUS recognizes more features than ERM, including horse back and muzzle, dog legs and tail, and phone body shape.

The Domain Generalization (DG) problem (Blanchard, Lee, and Scott 2011; Muandet, Balduzzi, and Schölkopf 2013) was introduced to address such cases. Specifically, a model trained on multiple source domains is expected to directly perform well in unseen target domains without requiring any exposure to its data. This problem setting can be interpreted as multi-source 0-shot domain adaptation.

Training a model to generalize across several related but unseen data distributions remains arguably one of the most challenging open problems in machine learning. In the last decade, a plethora of widely different methods were developed to address the DG problem. We refer to (Zhou et al.

2021a) for an extensive overview of DG algorithms. Despite these efforts, Gulrajani and Lopez-Paz found that carefully tuning the baseline, which simply applies Empirical Risk Minimization (ERM) on the data of the source domains, achieves a high performance that is competitive with state-of-the-art methods.

One major challenge of DG is that the model can only observe and learn features from the source domains, which may not be present in the unseen target domains, limiting generalization. We presume that learning a wider set of different features would increase the chance of learning features that are useful for a larger set of unseen domains. Hence, we introduce COLUMBUS, a training procedure for automated new feature discovery, which leads to a better feature recognition in unseen domains (Figure 1). During training on the source domains, COLUMBUS incentivizes the model to discover new features, even in data examples on which it already performs well. To achieve this, COLUMBUS prevents the model from using the features it deems most relevant for the source domains by corrupting them during training. To identify the most relevant features for a model, we leverage attribution methods (Tjoa and Guan 2020) usually used for model explainability purposes.

We evaluate our approach on the recently proposed DOMAINBED framework (Gulrajani and Lopez-Paz 2020) which includes several DG datasets and algorithm implementations to promote a fair and reproducible comparison of different approaches. Our method outperforms 18 DG algorithms evaluated on 3 datasets in the DOMAINBED framework, achieving new state-of-the-art results using 2 different model selection methods. Furthermore, our method achieves the highest performance when evaluated on unseen data from the source domains used for training (in-domain generalization), which confirms its effectiveness and ability to learn new features useful for unseen data.

2 Related Work

2.1 Domain Generalization

This section presents an overview of domain generalization (DG) approaches. Methods to which we compare in our experiments (Section 4) are highlighted in bold. We refer to (Zhou et al. 2021a) for an extensive overview of DG algorithms. The simplest approach to DG is to train one model via Empirical Risk Minimization (**ERM**) (Vapnik 1999) on the training datasets of all source domains. **GroupDRO** additionally increases the importance of source domains where the model yields a lower performance. In the following, we broadly categorize DG approaches into three categories.

Domain alignment methods aim to learn domain-invariant representations of the data by aligning features across the source domains. The reduction of the representation distribution mismatch across source domains can be achieved by minimizing the maximum mean discrepancy criteria (Gretton et al. 2012) combined with an adversarial autoencoder (**MMD**) (Li et al. 2018b), minimizing the difference between the means (Tzeng et al. 2014) or covariance matrices (**CORAL**) (Sun and Saenko 2016) in the embedding space across different domains, or minimizing a con-

trastive loss as a regularization (Motiian et al. 2017; Yoon, Hamarneh, and Garbi 2019; Mahajan, Tople, and Sharma 2020), e.g., **SelfReg** (Kim et al. 2021). The domain alignment is also addressed by promoting the loss gradient alignment across different domains via inner product maximization (**Fish**) (Shi et al. 2021) or binary (**AND-mask**) (Parascandolo et al. 2020; Shahtalebi et al. 2021) or continuous gradient masking (**SAND-mask**) (Shahtalebi et al. 2021).

Another line of works optimizes for features that confuse a domain discriminator model (Albuquerque et al. 2019; Shao et al. 2019; Rahman et al. 2020; Deng et al. 2020), and includes **DANN** (Ganin et al. 2016) and its class-conditional extension **C-DANN** (Li et al. 2018c). Other works additionally involve the classifier in the representation alignment, either by optimizing for an embedding space such that the optimal linear classifier on top of it is the same across different domains (**IRM**) (Arjovsky et al. 2019), or by passing a domain-specific mean embedding to the classifier as a second argument (**MTL**) (Blanchard et al. 2017). **VREx** (Krueger et al. 2021) is an approximation of IRM via a variance penalty and **ARM** (Zhang et al. 2020) is an extension of MTL that employs a separate embedding CNN.

Meta-learning techniques were also applied to DG by training a model in a bi-level optimization fashion on disjoint meta-train and meta-test sets sampled from the source domains. Hereby, **MLDG** (Li et al. 2018a) optimizes explicitly for parameters that can be quickly adapted to different domains, **MASF** (Dou et al. 2019) additionally employs inter-class and intra-class losses to regularize the embedding space, and **MetaReg** meta-learns a regularizer for the output layer (Balaji, Sankaranarayanan, and Chellappa 2018).

Data augmentation approaches were also proposed to tackle DG and our method falls into this category. Some works use **Mixup** (Zhang et al. 2017) to compute inter-domain examples to augment the training set (Xu et al. 2020; Yan et al. 2020; Wang, Li, and Kot 2020). **SagNets** (Nam et al. 2019) reduce style bias in an attempt to reduce domain gap by randomizing the style of images while keeping their content. Another line of works generate images by using adversarial attacks (Goodfellow, Shlens, and Szegedy 2014) to perturb input images based on a class classifier (Sinha et al. 2017; Volpi et al. 2018; Qiao, Zhao, and Peng 2020) or a domain classifier (Shankar et al. 2018), by training CNNs to synthesize images within the source domains (Rahman et al. 2019; Somavarapu, Ma, and Kira 2020; Borlino, D’Innocente, and Tommasi 2021) or novel domains (Maria Carlucci et al. 2019; Zhou et al. 2020a,b). Other works apply such perturbations on a feature level (Huang et al. 2020; Zhou et al. 2021b).

Our approach corrupts the raw input data as well as the multi-level representations that the model learns in order to enforce new feature discovery. Instead of using visually undetectable adversarial attacks or additional highly parametrized generative models, we employ attribution methods, e.g., Guided-Grad-CAM (Selvaraju et al. 2017), to identify and corrupt the most relevant features. Our approach shares similarities with **RSC** (Huang et al. 2020) which discards the most dominant features fed to the output layer to promote the activation of the remaining features.

The key difference of our approach is that we corrupt features not only in the last high-level representation space, i.e., the input to the output layer, but also in the raw input space and other low-level representation spaces. We argue that by discarding the features only in the representation space (e.g., elephant trunk detector), as done in RSC, the same silenced feature detectors can be relearned as long as the model is exposed to the corresponding features in the input space (e.g., the pixels of the elephant trunk). We hypothesize that corrupting the features in the input space is crucial to enforce the discovery of new features. Our empirical results show that our method outperforms RSC by a significant margin (Section 4) on unseen data from source and target domains, hence confirming our hypothesis.

2.2 Relevance Attribution

In an attempt to explain and interpret the predictions of deep learning models, several attribution methods that assign relevance scores to input features have been developed (Simonyan and Zisserman 2014; Selvaraju et al. 2017; Schurz et al. 2020). In Saliency Maps (Simonyan and Zisserman 2014) the relevance scores are given by the gradient of the output neuron corresponding to the ground truth w.r.t. the input. Better attributions were achieved by averaging these gradients over local neighborhood patches in SmoothGrad (Smilkov et al. 2017) and over brightness level interpolations in IntegratedGradients (Sundararajan, Taly, and Yan 2017). Another category of approaches modifies the back-propagation procedure by considering only positive gradients (Springenberg et al. 2014) or to satisfy the relevance conservation property through the layers (Bach et al. 2015; Montavon et al. 2017).

Class Activation Maps (CAM) (Zhou et al. 2016) leverages the activations in the last convolutional layer to produce a heatmap highlighting the relevance of each feature in the raw input. Gradient-weighted CAM (Grad-CAM) (Selvaraju et al. 2017) generalizes CAM to a variety of CNNs by using the gradient information flowing into the last convolutional layer. This method can be combined with GuidedBP (Springenberg et al. 2014) to yield GuidedGrad-CAM (Selvaraju et al. 2017). IBA (Schulz et al. 2020) approximates attribution scores by restricting the information flow via noise injection to intermediate feature maps during the forward pass.

While prior works employed attribution methods to explain and interpret model predictions, we leverage them for training purposes. To the best of our knowledge, we are the first to incorporate attribution methods combined with data corruption into training in order to improve the generalization ability of the model. For a broader overview of attribution methods, we refer to (Tjoa and Guan 2020).

3 Method

The proposed method improves the knowledge transfer to unknown data distributions by training a model to learn a rich set of features on several representation levels of the data via an automated new feature discovery.

Let F_s and F_t denote the sets of features learnable for the addressed classification task, which are present in

the data of the source domains and in the target domain, respectively, and G their intersection. In the optimal case, the set of features L learned by the model on the source domains encompasses G fully. Since F_t is unknown at training time, our method maximizes the size of L by training the model to learn as many features as possible, resulting in a higher chance to capture features from G via the higher intersection between L and G . To achieve this, we propose COLUMBUS, a training procedure that enables automated new feature discovery. COLUMBUS prevents the model from using (a part of) the most relevant features for its current predictions during training. This is done in 3 major steps: identification of the most relevant features, their corruption, and training with the corrupted data representations. Figure 2 presents an overview of our approach. We apply this technique on several levels of representations of the data ranging from the raw input, e.g., pixels of the elephant trunk, to the high-level features fed to the output layers, e.g., elephant-trunk-detector, including the representations yielded by intermediate layers, hence fostering multi-level new feature discovery.

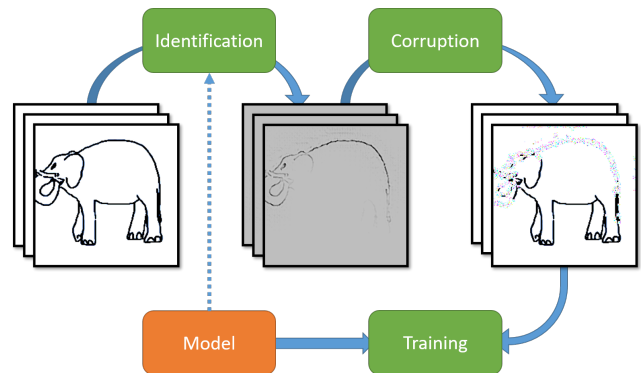


Figure 2: Overview of the proposed COLUMBUS method. In the identification stage, the most class-discriminative features according to the current model are identified via a relevance attribution method, which in this case is applied to the raw input representation. In the corruption stage, the identified features, e.g., elephant trunk and back, are perturbed by using a corruption method, in this case a replacement by a random pixel value was applied. Finally, the model is trained with the batch of corrupted data, promoting the discovery of new features, e.g., elephant feet and toes. The image used belongs to the PACS Sketch domain.

3.1 Identification

In each training iteration, we sample an attribution method from a set of attribution methods A , and use it to compute a relevance attribution map M that identifies the most relevant features. Any attribution method could be included in the set A . In this work, we use Saliency Maps (Simonyan and Zisserman 2014) and GuidedGrad-CAM (Selvaraju et al. 2017), since they are simple, fast, and model-architecture-agnostic. Other methods require modifications to support skip con-

nections and batch normalization layers (Bach et al. 2015), or involve training additional parameters after every model update (Schulz et al. 2020). Moreover, GuidedGrad-CAM was found to be competitive with state-of-the-art attribution methods in the image degradation evaluation (Schulz et al. 2020).

While Saliency Maps and GuidedGrad-CAM were developed to assign relevance scores to features in the input space, we extend their usage to identify relevant features in representations extracted by intermediate layers. Let \mathbf{y} and $\hat{\mathbf{y}}$ denote the ground truth and the model prediction for a data-point \mathbf{X} . The attribution map M_l yielded by Saliency Maps for a representation R_l yielded by layer l is given by

$$M_{l,Saliency} = \frac{\partial(\hat{\mathbf{y}} \odot \mathbf{y})}{\partial R_l}. \quad (1)$$

Note that the original Saliency Maps method (Simonyan and Zisserman 2014) corresponds to the case where $l = 0$, i.e., R_0 is the raw input representation.

The class-discriminative relevance map M_l yielded by Grad-CAM (Selvaraju et al. 2017) for a layer l is given by a sum over the channels of the representation R_l weighted by importance factors α_c for each channel c , resulting in

$$M_{l,GradCAM} = ReLU\left(\sum_c \alpha_c R_l^c\right). \quad (2)$$

Hereby, the importance factors are given by the gradient of the model prediction for the correct class w.r.t. the global-average-pooled representation R_l . Formally,

$$\alpha_c = \frac{1}{Z} \sum_i \sum_j \frac{\partial(\hat{\mathbf{y}} \odot \mathbf{y})}{\partial R_l^{c,i,j}}. \quad (3)$$

To assign relevance scores to features in the input space, Grad-CAM is applied to the representation yielded by the last convolutional layer to obtain a relevance map M which is then upsampled via bilinear interpolation to the input data size (Selvaraju et al. 2017). To identify the most relevant features in an intermediate representation R_l , we directly use the corresponding relevance map M_l (Equation 2). In our experiments, we use GuidedGrad-CAM (Selvaraju et al. 2017) which yields more fine-grained relevance maps than Grad-CAM by multiplying $M_{l,GradCAM}$ with the relevance maps determined by Guided Backpropagation (Guided BP) (Springenberg et al. 2014), for the same representation R_l . Guided BP modifies Saliency Maps by removing negative gradients when backpropagating through ReLU layers.

3.2 Corruption

In each training iteration, we sample a corruption method from the set of corruption methods C and use it to corrupt the identified most relevant features based on the relevance attribution map M . Any technique that perturbs the information contained in the identified features can be used. We use different corruption methods depending on the sampled representation level l .

To corrupt the raw input ($l = 0$), the most relevant input features according to the attribution map M_0 , e.g., the pixels corresponding to an elephant trunk, are perturbed using

a corruption method. Hereby, we perturb the identified pixel values by setting them to a random value, to zero, i.e., black pixels, by applying the Fast Gradient Sign Method (FGSM) (Goodfellow, Shlens, and Szegedy 2014), or by applying Gaussian blurring.

For an intermediate representation level $l > 0$, first the original input is fed through the model up to the corresponding layer l to yield the representation R_l . The latter is then corrupted based on the relevance attribution map M_l resulting from the identification stage and finally fed to the next layer. To corrupt intermediate embeddings, we drop the most relevant features, i.e., set their values to zero. This can be viewed as a targeted Dropout (Srivastava et al. 2014).

3.3 Training

The COLUMBUS training procedure is described by Algorithm 1. In each training iteration, a data batch B , a representation level l , a relevance attribution method, and a corruption method are sampled. Subsequently, the aforementioned identification and corruption steps are performed. The model is trained on the corrupted data (representations). Hereby, the $p\%$ most relevant features are corrupted. To enable the model to learn some features at the beginning of training, p is set to 0, i.e., no corruption is applied. As training progresses, more features are corrupted in the data, forcing the model to discover and learn new features. Concretely, p is linearly increased, throughout the training, to reach p_{max} , a hyperparameter. Note that the resulting gradual learning of new features, independently from each other, promotes also feature disentanglement, which was found to be beneficial for visual reasoning (van Steenkiste et al. 2019). We use different identification and corruption methods to increase the diversity of the corrupted data examples used to train the model and prevent overfitting. We also found that sampling multiple methods leads to better empirical results. It should also be noted that COLUMBUS is adaptive to the model’s learning, since the identification step is model-state-specific. In other words, if the model *forgets* a set of features during training, these will not be identified (again), and hence will not be corrupted (again), which enables the model to relearn them.

The model parameters θ are updated by minimizing a loss function f using a gradient-based optimization algorithm, e.g., Adam (Kingma and Ba 2014). In algorithm 1, SGD is used for simplicity of notation. The loss function f used is a weighted sum comprising a classification loss L_{cls} and a domain-alignment regularization loss term L_{DA} . Formally,

$$f = L_{cls} + \lambda \sum_{i=1}^{N_s} \sum_{j=i+1}^{N_s} L_{DA}(i, j), \quad (4)$$

where λ denotes a weighting factor and N_s is the number of source domains used for training. We use the cross-entropy loss as classification loss L_{cls} . L_{DA} regularizes the embedding space by minimizing the Frobenius norm between the domain-specific embedding means and covariance matrices for each pair of source domains i and j , as done in DDC

(Tzeng et al. 2014) and CORAL (Sun and Saenko 2016) respectively. The normalization of the regularization loss by the number of source domain pairs is omitted in Equation 4 for simplicity of notation. It should be noted that, unlike prior works (Tzeng et al. 2014; Sun and Saenko 2016; Gulrajani and Lopez-Paz 2020) that apply this loss on the representations of the original images, we use corrupted images and representations. This leads to an alignment in the embedding space not only across the domains, but also between the class-specific features, e.g., by minimizing the difference between the embedding distribution of cartoon images of elephant feet and art painting images of elephant trunks.

Algorithm 1: The COLUMBUS training procedure

Require: D_s : Training data of all source domains
Require: f : Loss function
Require: α : Learning rate
Require: L : Set of representation levels including the raw input level
Require: A : Set of relevance attribution methods
Require: C : Set of corruption methods
Require: p_{max} : Max. % of representation to be corrupted

- 1: Initialize the model parameters θ randomly or from a pre-trained model
- 2: Initialize the % of representation to be corrupted $p = 0$
- 3: **while** not done **do**
- 4: Sample a data batch $B = \{\mathbf{X}, \mathbf{y}\}$ from D_s
- 5: Sample level of representation l from L
- 6: Feed B through the model parametrized by θ
- 7: Get the relevance attribution map M_l by applying a relevance attribution method randomly sampled from A on level l using the current model parameters θ
- 8: **if** $l = 0$ **then**
- 9: Corrupt the values in B corresponding to the $p\%$ highest values in M_0 by applying a corruption method randomly sampled from C , yielding the corrupted input B_c
- 10: Feed B_c through the model to obtain the predictions $\hat{\mathbf{y}}$
- 11: **else**
- 12: Feed B through the model until level l to obtain the representation R_l
- 13: Corrupt the values in R_l corresponding to the $p\%$ highest values in M_l , yielding the corrupted representation $R_{l,c}$
- 14: Feed $R_{l,c}$ through the model starting from level $l + 1$ to obtain the predictions $\hat{\mathbf{y}}$
- 15: **end if**
- 16: Update θ : $\theta \leftarrow \theta - \alpha \nabla_{\theta} f(\mathbf{y}, \hat{\mathbf{y}})$
- 17: Increase p linearly towards p_{max}
- 18: **end while**
- 19: **return** Learned model parameters θ

In our experiments, we corrupt $q\%$ of the sampled data batch in each iteration, and increase q linearly during the training until q_{max} is reached, as done for the representation percentage to be corrupted p . This is omitted in Algorithm 1 for simplicity of notation. During training, we alternate be-

tween sampling an intermediate representation and the raw input for corruption. The intermediate representations correspond to the outputs of each ResNet block in the used ResNet-50 model (He et al. 2016). At test time, the model trained with COLUMBUS is applied to the data from the target domains without any corruption.

4 Experiments

4.1 Experimental Setup

The conducted experiments¹ aim to address the following key questions: (a) Can COLUMBUS achieve a higher DG performance than the simple but strong baseline ERM (Gulrajani and Lopez-Paz 2020), which simply trains the model on the source domains, and how does it compare to the state-of-the-art DG methods? (b) Does learning a richer set of features with COLUMBUS lead to a performance increase on unseen data from the source domains? (c) How much does the embeddings space regularization loss L_{DA} impact the performance of COLUMBUS?

We evaluate our approach on the recently proposed DOMAINBED framework (Gulrajani and Lopez-Paz 2020) which includes several DG datasets, implementations of DG algorithms, and model selection methods. DOMAINBED promotes a fair and reproducible comparison of the different approaches by including a common automated hyperparameter search, i.e., a random search with the given seeds conducts the same experiments for all methods. For a fair comparison with the 18 DG algorithms, our experiments follow the same experimental setting adopted in DOMAINBED (Gulrajani and Lopez-Paz 2020): We use a ResNet-50 model (He et al. 2016) pre-trained on ImageNet (Russakovsky et al. 2015) with frozen batch normalization (Ioffe and Szegedy 2015) statistics as suggested in (Seo et al. 2020), the same optimization algorithm, data augmentation techniques and number of training iterations used in DOMAINBED. The COLUMBUS-specific hyperparameters p_{max} , q_{max} and λ are included in the hyperparameter search of DOMAINBED, and the intervals used can be found in the Appendix.

We conduct experiments on 3 challenging multi-domain datasets commonly used as DG benchmarks: VLCS (Fang, Xu, and Rockmore 2013), OfficeHome (Venkateswara et al. 2017) and PACS (Li et al. 2017). VLCS contains images belonging to 5 classes from 4 photographic domains: VOC2007 (V), LabelMe (L), Caltech101 (C), and SUN09 (S). OfficeHome consists of images of 65 classes from the domains Art (A), Clipart (C), Product (P), and Real (R). PACS comprises images belonging to 7 classes from the domains Art-painting (A), Cartoon (C), Photo (P), and Sketch (S). DOMAINBED splits the data from each source domain into 80% for training and 20% for validation. Each experiment is repeated 3 times with the provided seeds.

4.2 Results

In this section, we present the results of the experiments conducted to answer our questions (Section 4.1). First, we present the domain generalization results achieved by

¹Code will be made public upon paper acceptance.

COLUMBUS and the baselines on DOMAINBED, using two different DG selection methods. Subsequently, we demonstrate the effectiveness of our approach on in-domain generalization. Finally, we assess the impact of removing the domain alignment regularization loss, by evaluating a *non-regularized* version of our approach (NR-COLUMBUS).

Domain Generalization Tables 1, 2 and 3 show the results averaged over the 3 seeds pre-determined by DOMAINBED, on VLCS, PACS and OfficeHome respectively. Hereby, the unseen target domain is defined by the column name, i.e., the 3 other domains are used as source domains for model training. The test accuracy is computed on the test set of the target domain. The complete results including standard deviations can be found in the appendix. The average results over the domains of each dataset can be seen in Table 4. We select the model with the highest source-domain validation performance for the evaluation on the target domain.

Algorithm	C	L	S	V	Avg
ERM	97.7	64.3	73.4	74.6	77.5
IRM	98.6	64.9	73.4	77.3	78.5
GroupDRO	97.3	63.4	69.5	76.7	76.7
Mixup	98.3	64.8	72.1	74.3	77.4
MLDG	97.4	65.2	71.0	75.3	77.2
CORAL	98.3	66.1	73.4	77.5	78.8
MMD	97.7	64.0	72.8	75.3	77.5
DANN	99.0	65.1	73.1	77.2	78.6
CDANN	97.1	65.1	70.7	77.1	77.5
MTL	97.8	64.3	71.5	75.3	77.2
SagNet	97.9	64.5	71.4	77.5	77.8
ARM	98.7	63.6	71.3	76.7	77.6
VREx	98.4	64.4	74.1	76.2	78.3
RSC	97.9	62.5	72.3	75.6	77.1
NR-COLUMBUS	99.0	63.0	74.4	78.6	78.7
COLUMBUS	98.8	63.8	72.7	78.9	78.6

Table 1: Domain Generalization results on VLCS.

Algorithm	A	C	P	S	Avg
ERM	84.7	80.8	97.2	79.3	85.5
IRM	84.8	76.4	96.7	76.1	83.5
GroupDRO	83.5	79.1	96.7	78.3	84.4
Mixup	86.1	78.9	97.6	75.8	84.6
MLDG	85.5	80.1	97.4	76.6	84.9
CORAL	88.3	80.0	97.5	78.8	86.2
MMD	86.1	79.4	96.6	76.5	84.6
DANN	86.4	77.4	97.3	73.5	83.6
CDANN	84.6	75.5	96.8	73.5	82.6
MTL	87.5	77.1	96.4	77.3	84.6
SagNet	87.4	80.7	97.1	80.0	86.3
ARM	86.8	76.8	97.4	79.3	85.1
VREx	86.0	79.1	96.9	77.7	84.9
RSC	85.4	79.7	97.6	78.2	85.2
NR-COLUMBUS	88.3	79.3	97.3	81.5	86.6
COLUMBUS	90.3	79.6	97.1	81.8	87.2

Table 2: Domain Generalization results on PACS.

Algorithm	A	C	P	R	Avg
ERM	61.3	52.4	75.8	76.6	66.5
IRM	58.9	52.2	72.1	74.0	64.3
GroupDRO	60.4	52.7	75.0	76.0	66.0
Mixup	62.4	54.8	76.9	78.3	68.1
MLDG	61.5	53.2	75.0	77.5	66.8
CORAL	65.3	54.4	76.5	78.4	68.7
MMD	60.4	53.3	74.3	77.4	66.3
DANN	59.9	53.0	73.6	76.9	65.9
CDANN	61.5	50.4	74.4	76.6	65.8
MTL	61.5	52.4	74.9	76.8	66.4
SagNet	63.4	54.8	75.8	78.3	68.1
ARM	58.9	51.0	74.1	75.2	64.8
VREx	60.7	53.0	75.3	76.6	66.4
RSC	60.7	51.4	74.8	75.1	65.5
NR-COLUMBUS	61.6	58.4	75.4	77.5	68.2
COLUMBUS	64.3	60.6	76.5	78.8	70.1

Table 3: Domain generalization results on OfficeHome.

COLUMBUS achieves the highest results on all datasets on average, advancing the state-of-the-art by 2.1% and 0.7% compared to ERM and the best baseline respectively. We note an impressive 8.2% improvement on OfficeHome’s most challenging domain *Clipart* (C) compared to ERM and almost 6% compared to the best baseline, on this 65-class classification task. Likewise, on the Art-painting domain of PACS, a substantial 8.2% and 2% increases are observed compared to ERM and the best baseline respectively. Significant increases of 2.5% and 1.8% were also achieved on PACS’s challenging *Sketch* (S) domain, compared to ERM and the best baseline. On all target domains, COLUMBUS consistently outperforms all the baselines or yields a competitive performance. The fact that COLUMBUS outperforms RSC (Huang et al. 2020) confirms our hypothesis, that corrupting the learned features in the raw input is crucial to prevent relearning the same high-level features, and hence enforce new feature discovery.

We also evaluated our approach using the oracle selection method proposed in (Gulrajani and Lopez-Paz 2020), where the model is evaluated on a held-out validation set from the target domain. In order to limit access to the target domain, this evaluation is performed only once at the end of each training run, disallowing early stopping. The average results on the 3 datasets are presented in Table 5.

When using the oracle selection method, the performance gap between COLUMBUS and the best performing baseline CORAL almost doubles compared to using the training domain validation set selection method, increasing from 0.7% to 1.3%. This shows that the performance advantage of COLUMBUS is increased when better proxies for model selection, e.g., a held-out set from the target domain, are available, further confirming the effectiveness of our approach. Our results on DOMAINBED using both model selection methods show that the additional features learned thanks to the corruption of the most relevant features are useful for

Algorithm	VLCS	PACS	OfficeHome	Avg
ERM	77.5 ± 0.4	85.5 ± 0.2	66.5 ± 0.3	76.5
IRM	78.5 ± 0.5	83.5 ± 0.8	64.3 ± 2.2	75.5
GroupDRO	76.7 ± 0.6	84.4 ± 0.8	66.0 ± 0.7	75.7
Mixup	77.4 ± 0.6	84.6 ± 0.6	68.1 ± 0.3	76.7
MLDG	77.2 ± 0.4	84.9 ± 1.0	66.8 ± 0.6	76.3
CORAL	78.8 ± 0.6	86.2 ± 0.3	68.7 ± 0.3	77.9
MMD	77.5 ± 0.9	84.6 ± 0.5	66.3 ± 0.1	76.2
DANN	78.6 ± 0.4	83.6 ± 0.4	65.9 ± 0.6	76.0
CDANN	77.5 ± 0.1	82.6 ± 0.9	65.8 ± 1.3	75.3
MTL	77.2 ± 0.4	84.6 ± 0.5	66.4 ± 0.5	76.1
SagNet	77.8 ± 0.5	86.3 ± 0.2	68.1 ± 0.1	77.4
ARM	77.6 ± 0.3	85.1 ± 0.4	64.8 ± 0.3	75.8
VREx	78.3 ± 0.2	84.9 ± 0.6	66.4 ± 0.6	76.5
RSC	77.1 ± 0.5	85.2 ± 0.9	65.5 ± 0.9	75.9
SelfReg	77.8 ± 0.9	85.6 ± 0.4	67.9 ± 0.7	77.1
Fish	77.8 ± 0.3	85.5 ± 0.3	68.6 ± 0.4	77.3
AND-mask	78.1 ± 0.9	84.4 ± 0.9	65.6 ± 0.4	76.0
SAND-mask	77.4 ± 0.2	84.6 ± 0.9	65.8 ± 0.4	75.9
NR-COLUMBUS	78.7 ± 0.3	86.6 ± 0.1	68.2 ± 0.2	77.8
COLUMBUS	78.6 ± 0.5	87.2 ± 0.2	70.1 ± 0.3	78.6

Table 4: Average domain generalization results.

generalization to unseen domains. This is backed by Figure 1, where COLUMBUS recognizes more features in the unseen target domain than ERM.

Source Domain Generalization In this section, we investigate whether the richer set of features learned by COLUMBUS leads to a better in-domain generalization, i.e., whether a performance boost is also yielded on unseen data from the source domains used for training. We evaluate COLUMBUS and the DG baselines on the held-out validation sets of the source domains and report the maximal average validation accuracy across domains in Table 6².

COLUMBUS consistently achieves the highest validation performance on the training domains compared to the DG baselines, on every dataset. This shows that the richer set of learned features improves generalization to unseen in-distribution data examples as well, suggesting that COLUMBUS might be suitable for applications beyond domain generalization to include scenarios without domain shift.

Ablation Study Finally, we conduct a small ablation study to assess the impact of the domain alignment regularization loss term L_{DA} . For that, we evaluate a *non-regularized* version of COLUMBUS, i.e., $\lambda = 0$, to which refer as NR-COLUMBUS, in the same experimental setting. The results can be seen in Tables 1-6.

We find that, on average, the regularization yields a performance increase for in-domain and out-of-domain generalization, using both selection methods. Only on VLCS, it leads to a marginal (0.1%) performance decrease. In comparison to the DG baselines, NR-COLUMBUS still outperforms all the other methods in in-domain generalization and domain generalization using the oracle selection method.

²For the baselines, we computed the results using the logs made public in <https://drive.google.com/file/d/16VFQWTble6-nB5AdXbtQpQFwjEC7CChM/view?usp=sharing>.

Algorithm	VLCS	PACS	OfficeHome	Avg
ERM	77.6 ± 0.3	86.7 ± 0.3	66.4 ± 0.5	76.9
IRM	76.9 ± 0.6	84.5 ± 1.1	63.0 ± 2.7	74.8
GroupDRO	77.4 ± 0.5	87.1 ± 0.1	66.2 ± 0.6	76.9
Mixup	78.1 ± 0.3	86.8 ± 0.3	68.0 ± 0.2	77.6
MLDG	77.5 ± 0.1	86.8 ± 0.4	66.6 ± 0.3	77.0
CORAL	77.7 ± 0.2	87.1 ± 0.5	68.4 ± 0.2	77.7
MMD	77.9 ± 0.1	87.2 ± 0.1	66.2 ± 0.3	77.1
DANN	79.7 ± 0.5	85.2 ± 0.2	65.3 ± 0.8	76.8
CDANN	79.9 ± 0.2	85.8 ± 0.8	65.3 ± 0.5	77.0
MTL	77.7 ± 0.5	86.7 ± 0.2	66.5 ± 0.4	77.0
SagNet	77.6 ± 0.1	86.4 ± 0.4	67.5 ± 0.2	77.2
ARM	77.8 ± 0.3	85.8 ± 0.2	64.8 ± 0.4	76.1
VREx	78.1 ± 0.2	87.2 ± 0.6	65.7 ± 0.3	77.0
RSC	77.8 ± 0.6	86.2 ± 0.5	66.5 ± 0.6	76.8
AND-mask	76.4 ± 0.4	86.4 ± 0.4	66.1 ± 0.2	76.3
SAND-mask	76.2 ± 0.5	85.9 ± 0.4	65.9 ± 0.5	76.0
NR-COLUMBUS	79.2 ± 0.2	87.9 ± 0.3	68.4 ± 0.2	78.5
COLUMBUS	79.0 ± 0.4	88.0 ± 0.2	70.0 ± 0.3	79.0

Table 5: Domain Generalization results using the test-domain validation set (oracle) as a selection method.

Algorithm	VLCS	PACS	OfficeHome	Avg
ERM	86.4 ± 0.0	97.0 ± 0.1	82.1 ± 0.2	88.5
IRM	85.8 ± 0.2	96.5 ± 0.4	79.9 ± 2.0	87.4
GroupDRO	86.4 ± 0.0	96.9 ± 0.1	81.6 ± 0.2	88.3
Mixup	86.6 ± 0.1	97.4 ± 0.1	83.2 ± 0.3	89.0
MLDG	86.4 ± 0.1	97.1 ± 0.1	82.4 ± 0.3	88.6
CORAL	86.5 ± 0.0	97.1 ± 0.1	83.7 ± 0.2	89.1
MMD	86.4 ± 0.1	96.9 ± 0.0	82.0 ± 0.1	88.4
DANN	86.3 ± 0.0	96.4 ± 0.3	80.4 ± 0.9	87.7
CDANN	86.4 ± 0.1	96.4 ± 0.3	80.5 ± 0.9	87.8
MTL	86.3 ± 0.0	97.0 ± 0.0	81.7 ± 0.2	88.3
SagNet	86.4 ± 0.0	97.0 ± 0.2	82.9 ± 0.4	88.8
ARM	86.3 ± 0.0	96.5 ± 0.1	80.2 ± 0.2	87.7
VREx	86.2 ± 0.1	96.9 ± 0.1	81.8 ± 0.4	88.3
RSC	86.4 ± 0.3	96.8 ± 0.2	81.5 ± 0.3	88.2
NR-COLUMBUS	86.8 ± 0.1	97.4 ± 0.1	83.2 ± 0.2	89.2
COLUMBUS	86.7 ± 0.1	97.6 ± 0.0	84.0 ± 0.3	89.4

Table 6: Source domain validation performance.

5 Conclusion

In this work, we proposed COLUMBUS, a novel and strong domain generalization (DG) approach that enforces new feature discovery to improve the transfer to a wider set of unseen domains. During training, COLUMBUS corrupts the input and multi-level representations of the data most relevant for the model. For the identification of such features, relevance attribution methods that are usually used for model explainability purposes are leveraged. Our extensive empirical evaluation on DOMAINBED demonstrates the effectiveness of the proposed method, which outperforms 18 DG algorithms and achieves new state-of-the-art results on multiple DG benchmarks. Our results show that the richer set of learned features improves the generalization to unseen data from both seen and unseen domains, suggesting the suitability of our approach for applications beyond domain generalization to include scenarios without domain shift.

References

- Albuquerque, I.; Monteiro, J.; Darvishi, M.; Falk, T. H.; and Mitliagkas, I. 2019. Generalizing to unseen domains via distribution matching. *arXiv:1911.00804*.
- Alcorn, M. A.; Li, Q.; Gong, Z.; Wang, C.; Mai, L.; Ku, W.-S.; and Nguyen, A. 2019. Strike (with) a pose: Neural networks are easily fooled by strange poses of familiar objects. In *IEEE/CVF CVPR*.
- Arjovsky, M.; Bottou, L.; Gulrajani, I.; and Lopez-Paz, D. 2019. Invariant risk minimization. *arXiv:1907.02893*.
- Bach, S.; Binder, A.; Montavon, G.; Klauschen, F.; Müller, K.-R.; and Samek, W. 2015. On pixel-wise explanations for non-linear classifier decisions by layer-wise relevance propagation. *PloS one*.
- Balaji, Y.; Sankaranarayanan, S.; and Chellappa, R. 2018. Metareg: Towards domain generalization using meta-regularization. *NeurIPS*.
- Blanchard, G.; Deshmukh, A. A.; Dogan, U.; Lee, G.; and Scott, C. 2017. Domain generalization by marginal transfer learning. *arXiv:1711.07910*.
- Blanchard, G.; Lee, G.; and Scott, C. 2011. Generalizing from several related classification tasks to a new unlabeled sample. *NeurIPS*.
- Borlino, F. C.; D’Innocente, A.; and Tommasi, T. 2021. Rethinking domain generalization baselines. In *International Conference on Pattern Recognition (ICPR)*.
- Deng, Z.; Ding, F.; Dwork, C.; Hong, R.; Parmigiani, G.; Patil, P.; and Sur, P. 2020. Representation via representations: Domain generalization via adversarially learned invariant representations. *arXiv:2006.11478*.
- Dou, Q.; Coelho de Castro, D.; Kamnitsas, K.; and Glocker, B. 2019. Domain generalization via model-agnostic learning of semantic features. *NeurIPS*.
- Fang, C.; Xu, Y.; and Rockmore, D. N. 2013. Unbiased metric learning: On the utilization of multiple datasets and web images for softening bias. In *IEEE ICCV*.
- Ganin, Y.; Ustinova, E.; Ajakan, H.; Germain, P.; Larochelle, H.; Laviolette, F.; Marchand, M.; and Lempitsky, V. 2016. Domain-adversarial training of neural networks. *JMLR*.
- Goodfellow, I. J.; Shlens, J.; and Szegedy, C. 2014. Explaining and harnessing adversarial examples. *arXiv:1412.6572*.
- Gretton, A.; Borgwardt, K. M.; Rasch, M. J.; Schölkopf, B.; and Smola, A. 2012. A kernel two-sample test. *JMLR*.
- Gulrajani, I.; and Lopez-Paz, D. 2020. In search of lost domain generalization. *arXiv:2007.01434*.
- He, K.; Zhang, X.; Ren, S.; and Sun, J. 2016. Deep residual learning for image recognition. In *IEEE CVPR*.
- Huang, Z.; Wang, H.; Xing, E. P.; and Huang, D. 2020. Self-challenging improves cross-domain generalization. In *Computer Vision—ECCV 2020: 16th European Conference*.
- Ioffe, S.; and Szegedy, C. 2015. Batch normalization: Accelerating deep network training by reducing internal covariate shift. In *ICML*.
- Kim, D.; Park, S.; Kim, J.; and Lee, J. 2021. SelfReg: Self-supervised Contrastive Regularization for Domain Generalization. *arXiv:2104.09841*.
- Kingma, D. P.; and Ba, J. 2014. Adam: A method for stochastic optimization. *arXiv:1412.6980*.
- Krueger, D.; Caballero, E.; Jacobsen, J.-H.; Zhang, A.; Binas, J.; Zhang, D.; Le Priol, R.; and Courville, A. 2021. Out-of-distribution generalization via risk extrapolation (rex). In *ICML*.
- Li, D.; Yang, Y.; Song, Y.-Z.; and Hospedales, T. M. 2017. Deeper, broader and artier domain generalization. In *IEEE ICCV*.
- Li, D.; Yang, Y.; Song, Y.-Z.; and Hospedales, T. M. 2018a. Learning to generalize: Meta-learning for domain generalization. In *AAAI Conference on Artificial Intelligence*.
- Li, H.; Pan, S. J.; Wang, S.; and Kot, A. C. 2018b. Domain generalization with adversarial feature learning. In *IEEE CVPR*.
- Li, Y.; Tian, X.; Gong, M.; Liu, Y.; Liu, T.; Zhang, K.; and Tao, D. 2018c. Deep domain generalization via conditional invariant adversarial networks. In *ECCV*.
- Mahajan, D.; Tople, S.; and Sharma, A. 2020. Domain generalization using causal matching. *arXiv:2006.07500*.
- Maria Carlucci, F.; Russo, P.; Tommasi, T.; and Caputo, B. 2019. Hallucinating agnostic images to generalize across domains. In *IEEE/CVF ICCV Workshops*.
- Montavon, G.; Lapuschkin, S.; Binder, A.; Samek, W.; and Müller, K.-R. 2017. Explaining nonlinear classification decisions with deep Taylor decomposition. *Pattern Recognition*.
- Motiian, S.; Piccirilli, M.; Adjero, D. A.; and Doretto, G. 2017. Unified deep supervised domain adaptation and generalization. In *IEEE ICCV*.
- Muandet, K.; Balduzzi, D.; and Schölkopf, B. 2013. Domain generalization via invariant feature representation. In *ICML*.
- Nam, H.; Lee, H.; Park, J.; Yoon, W.; and Yoo, D. 2019. Reducing domain gap via style-agnostic networks. *arXiv e-prints*.
- Parascandolo, G.; Neitz, A.; Orvieto, A.; Gresele, L.; and Schölkopf, B. 2020. Learning explanations that are hard to vary. *arXiv:2009.00329*.
- Qiao, F.; Zhao, L.; and Peng, X. 2020. Learning to learn single domain generalization. In *IEEE/CVF CVPR*.
- Rahman, M. M.; Fookes, C.; Baktashmotlagh, M.; and Sridharan, S. 2019. Multi-component image translation for deep domain generalization. In *2019 IEEE Winter Conference on Applications of Computer Vision (WACV)*.
- Rahman, M. M.; Fookes, C.; Baktashmotlagh, M.; and Sridharan, S. 2020. Correlation-aware adversarial domain adaptation and generalization. *Pattern Recognition*.
- Russakovsky, O.; Deng, J.; Su, H.; Krause, J.; Satheesh, S.; Ma, S.; Huang, Z.; Karpathy, A.; Khosla, A.; Bernstein, M.; et al. 2015. Imagenet large scale visual recognition challenge. *International journal of computer vision*.

- Schulz, K.; Sixt, L.; Tombari, F.; and Landgraf, T. 2020. Restricting the flow: Information bottlenecks for attribution. *arXiv:2001.00396*.
- Selvaraju, R. R.; Cogswell, M.; Das, A.; Vedantam, R.; Parikh, D.; and Batra, D. 2017. Grad-cam: Visual explanations from deep networks via gradient-based localization. In *IEEE ICCV*.
- Seo, S.; Suh, Y.; Kim, D.; Kim, G.; Han, J.; and Han, B. 2020. Learning to optimize domain specific normalization for domain generalization. In *ECCV*.
- Shahtalebi, S.; Gagnon-Audet, J.-C.; Laleh, T.; Faramarzi, M.; Ahuja, K.; and Rish, I. 2021. SAND-mask: An Enhanced Gradient Masking Strategy for the Discovery of Invariances in Domain Generalization. *arXiv:2106.02266*.
- Shankar, S.; Piratla, V.; Chakrabarti, S.; Chaudhuri, S.; Jyothi, P.; and Sarawagi, S. 2018. Generalizing across domains via cross-gradient training. *arXiv:1804.10745*.
- Shao, R.; Lan, X.; Li, J.; and Yuen, P. C. 2019. Multi-adversarial discriminative deep domain generalization for face presentation attack detection. In *IEEE/CVF CVPR*.
- Shi, Y.; Seely, J.; Torr, P. H.; Siddharth, N.; Hannun, A.; Usunier, N.; and Synnaeve, G. 2021. Gradient Matching for Domain Generalization. *arXiv:2104.09937*.
- Simonyan, K.; and Zisserman, A. 2014. Very deep convolutional networks for large-scale image recognition. *arXiv:1409.1556*.
- Sinha, A.; Namkoong, H.; Volpi, R.; and Duchi, J. 2017. Certifying some distributional robustness with principled adversarial training. *arXiv:1710.10571*.
- Smilkov, D.; Thorat, N.; Kim, B.; Viégas, F.; and Wattenberg, M. 2017. Smoothgrad: removing noise by adding noise. *arXiv:1706.03825*.
- Somavarapu, N.; Ma, C.-Y.; and Kira, Z. 2020. Frustratingly simple domain generalization via image stylization. *arXiv:2006.11207*.
- Springenberg, J. T.; Dosovitskiy, A.; Brox, T.; and Riedmiller, M. 2014. Striving for simplicity: The all convolutional net. *arXiv:1412.6806*.
- Srivastava, N.; Hinton, G.; Krizhevsky, A.; Sutskever, I.; and Salakhutdinov, R. 2014. Dropout: a simple way to prevent neural networks from overfitting. *JMLR*.
- Sun, B.; and Saenko, K. 2016. Deep coral: Correlation alignment for deep domain adaptation. In *ECCV*.
- Sundararajan, M.; Taly, A.; and Yan, Q. 2017. Axiomatic attribution for deep networks. In *ICML*.
- Tjoa, E.; and Guan, C. 2020. A survey on explainable artificial intelligence (xai): Toward medical xai. *IEEE Transactions on Neural Networks and Learning Systems*.
- Tzeng, E.; Hoffman, J.; Zhang, N.; Saenko, K.; and Darrell, T. 2014. Deep domain confusion: Maximizing for domain invariance. *arXiv:1412.3474*.
- van Steenkiste, S.; Locatello, F.; Schmidhuber, J.; and Bachem, O. 2019. Are disentangled representations helpful for abstract visual reasoning? *arXiv:1905.12506*.
- Vapnik, V. N. 1999. An overview of statistical learning theory. *IEEE transactions on neural networks*.
- Venkateswara, H.; Eusebio, J.; Chakraborty, S.; and Panchanathan, S. 2017. Deep hashing network for unsupervised domain adaptation. In *IEEE CVPR*.
- Volpi, R.; Namkoong, H.; Sener, O.; Duchi, J.; Murino, V.; and Savarese, S. 2018. Generalizing to unseen domains via adversarial data augmentation. *arXiv:1805.12018*.
- Wang, M.; and Deng, W. 2018. Deep visual domain adaptation: A survey. *Neurocomputing*.
- Wang, Y.; Li, H.; and Kot, A. C. 2020. Heterogeneous domain generalization via domain mixup. In *IEEE International Conference on Acoustics, Speech and Signal Processing (ICASSP)*.
- Wilson, G.; and Cook, D. J. 2020. A survey of unsupervised deep domain adaptation. *ACM Transactions on Intelligent Systems and Technology (TIST)*.
- Xu, M.; Zhang, J.; Ni, B.; Li, T.; Wang, C.; Tian, Q.; and Zhang, W. 2020. Adversarial domain adaptation with domain mixup. In *AAAI Conference on Artificial Intelligence*.
- Yan, S.; Song, H.; Li, N.; Zou, L.; and Ren, L. 2020. Improve unsupervised domain adaptation with mixup training. *arXiv:2001.00677*.
- Yoon, C.; Hamarneh, G.; and Garbi, R. 2019. Generalizable feature learning in the presence of data bias and domain class imbalance with application to skin lesion classification. In *International Conference on Medical Image Computing and Computer-Assisted Intervention*.
- Yue, X.; Zhang, Y.; Zhao, S.; Sangiovanni-Vincentelli, A.; Keutzer, K.; and Gong, B. 2019. Domain randomization and pyramid consistency: Simulation-to-real generalization without accessing target domain data. In *IEEE/CVF ICCV*.
- Zhang, H.; Cisse, M.; Dauphin, Y. N.; and Lopez-Paz, D. 2017. mixup: Beyond empirical risk minimization. *arXiv:1710.09412*.
- Zhang, M.; Marklund, H.; Dhawan, N.; Gupta, A.; Levine, S.; and Finn, C. 2020. Adaptive risk minimization: A meta-learning approach for tackling group distribution shift. *arXiv:2007.02931*.
- Zhou, B.; Khosla, A.; Lapedriza, A.; Oliva, A.; and Torralba, A. 2016. Learning deep features for discriminative localization. In *IEEE CVPR*.
- Zhou, K.; Liu, Z.; Qiao, Y.; Xiang, T.; and Loy, C. C. 2021a. Domain generalization: A survey. *arXiv:2103.02503*.
- Zhou, K.; Yang, Y.; Hospedales, T.; and Xiang, T. 2020a. Deep domain-adversarial image generation for domain generalisation. In *AAAI Conference on Artificial Intelligence*.
- Zhou, K.; Yang, Y.; Hospedales, T.; and Xiang, T. 2020b. Learning to generate novel domains for domain generalization. In *ECCV*.
- Zhou, K.; Yang, Y.; Qiao, Y.; and Xiang, T. 2021b. Domain generalization with mixstyle. *arXiv:2104.02008*.